Journal of the European Ceramic Society **17** (1997) 525–535

PII: S0955-2219(96)00095-7
0955-2219/97/$17.00

Thin Films by Consolidation and Sintering of Nanocrystalline Powders

X. Yang & M. N. Rahaman*

University of Missouri-Rolla, Department of Ceramic Engineering, Rolla, MI 65401, USA

(Received 19 December 1995; revised version received 15 May 1996; accepted 21 May 1996)

Abstract

Nanocrystalline CeO_2 and Y_2O_3-doped CeO_2 powders (particle size of 10–15 nm) were prepared under hydrothermal conditions at temperatures between 100 and 300°C. X-ray diffraction and transmission electron microscopy revealed that the particles were crystalline. The particle size distribution followed approximately the Lifshitz–Slyozov–Wagner theory for Ostwald ripening controlled by the diffusion step. Powder compacts were sintered to nearly full density below 1350°C. Thin adherent films (0·5 to 1 μm thick) on rigid substrates were prepared by spin-coating or dip-coating of stabilized suspensions, followed by drying and sintering. Dilute suspensions in aqueous solvents were stabilized electrostatically at pH values of 3·5 to 4. However, increasing particle concentration produced flocculation. Higher particle concentrations can be achieved without flocculation through the use of sterically stabilized suspensions with polyvinylpyrrolidone (PVP) as a dispersant. With these suspensions, homogeneous films were deposited on porous or dense substrates. The shrinkage kinetics of the adherent films were approximately the same as those for the powder compacts. The use of nanocrystalline powders offers a unique advantage for the production of adherent films with controlled microstructures on dense or porous substrates at relatively low temperatures. © *1997 Elsevier Science Limited. All rights reserved.*

1 Introduction

Polycrystalline ceramic thin films with controlled microstructure are required for many technological applications, including gas separation membranes,[1–3] solid oxide fuel cells,[4] and optoelectronic,[5] electrical[6] and magnetic[7] devices. A variety of techniques can be used to prepare adherent thin films with thicknesses in the range of a fraction of a micrometre to a few tens of micrometres. The techniques can be broadly classified into two categories: (i) vapour phase deposition and (ii) liquid-based methods. Vapour phase methods include chemical vapour deposition,[8] evaporation[9] and sputtering.[10] Liquid-based methods cover deposition by chemical reactions from solution (e.g. by homogeneous precipitation,[11] spray pyrolysis[12] or electrochemical reactions[13,14]), deposition from solutions or suspensions (e.g. by spin-coating or dip-coating), screen printing and liquid phase epitaxy.[15]

Liquid-based methods such as dip-coating or spin-coating of solutions are widely used for the preparation of ceramic thin films. A common method is the solution sol–gel process in which a solution of metal alkoxides or a solution of polymers is deposited on a substrate. The films normally consist of a polymeric structure in which the fine pores (typically less than 20–50 nm in diameter) are filled with liquid. The weak nature of the film coupled with the very large capillary stresses accompanying the evaporation of the liquid limits the thickness of the deposited film to less than ≈ 1 μm if cracking during the drying stage is to be prevented. Furthermore, the volume fraction of solids in the deposited film is typically less than 10% and the conversion of the polymeric structure to a ceramic results in a weight loss of greater than ≈20%. A dense film produced from a single coating in the sol–gel process is therefore typically less than 0·1 μm thick. Multiple coatings must be applied by repeating the deposition, drying and firing steps to produce a thicker film.[16,17]

Compared with the films produced by the solution sol–gel process, thicker films can be produced by dip-coating or spin-coating of suspensions of particles. However, the firing temperatures for the production of fairly dense films are considerably higher. The volume fraction of solids in the deposited film can be fairly high (up to 60–65%) and the capillary stresses developed during drying are significantly lower than those for films

*To whom correspondence should be addressed.

produced by the solution sol–gel process. For commonly available powders, the particle size is typically greater than 0·1 μm. Furthermore, the particles (grains) grow during sintering. If the thickness of the film is not greater than the average size of the grains, then desintering of the film may occur.[18] In practice, the thickness of the films produced from suspensions is normally greater than ≈ 10 μm.

The use of suspensions of nanocrystalline powders (particle size less than 10–20 nm) can yield significant advantages in the production of thin films. Because of the enhanced sinterability of the powders, lower firing temperatures can be used. Film thicknesses from a fraction of a μm to a few μm (i.e. thicknesses in the range between those achieved with the solution sol–gel process and suspensions of coarser powders) can be produced. However, the very fine particle size of nanocrystalline powders can present significant problems in the consolidation of the suspensions. It might be expected that relatively low particle concentrations would be achieved in the suspensions which can limit the homogeneity of the film.

Nanocrystalline powders have been produced by several techniques. Chemical vapour deposition has been used to synthesize SiC, Si_3N_4 and several oxides.[19,20] Recently, the inert gas condensation technique[21] has received considerable interest for the synthesis of nanocrystalline oxide powders. However, agglomeration during the oxidation step in the technique and during exposure to water vapour can limit the quality of the suspension when the powder is dispersed in liquids. Hydrothermal synthesis is an attractive method for the synthesis of nanocrystalline oxide powders. The process, involving precipitation from aqueous solution under conditions of elevated temperature and pressure, has been used for decades for the synthesis of very fine powders.[22,23] It facilitates good control of the particle characteristics (e.g. purity, average size and size distribution of the particles) and the incorporation of dopants uniformly into the powder. Furthermore, because the powders are produced in the aqueous solvent, the particles can remain dispersed in a liquid at all times prior to consolidation into a film. The elimination of any drying step significantly reduces the tendency for agglomeration of the powders. The well dispersed particles are expected to enhance the uniformity of the suspensions formed from the powder and, hence, the uniformity of the film produced from the suspension.

The work described in the present paper involved an investigation into the factors which control the synthesis of nanocrystalline powders by the hydrothermal technique, the stability of suspensions prepared from the synthesized powder and the sintering of thin films deposited on to rigid substrates by spin-coating of the suspensions. Powders of undoped CeO_2 and CeO_2 doped with 6 at% Y (for grain growth control[24]) were synthesized. Both electrostatic repulsion and steric repulsion were investigated for stabilization of the suspensions. The work is expected to be relevant not only to the basic science of processing nanocrystalline powders, but also to the application of CeO_2 thin films in fuel cells and other electronic devices.

2 Experimental Procedure

2.1 Hydrothermal synthesis and characterization of the CeO_2 powders and Y_2O_3-doped CeO_2 powders

Cerium nitrate hexahydrate, $Ce(NO_3)_3 \cdot 6H_2O$, and yttrium chloride hexahydrate, $YCl_3 \cdot 6H_2O$, were used as the starting materials. (Both chemicals, with a purity of 99·999%, were obtained from Aldrich Chemical Company, Milwaukee, WI.) In the preparation of the powder, the appropriate amounts of cerium nitrate (for the preparation of CeO_2) or cerium nitrate and yttrium chloride (for the CeO_2 powder doped with 6 at% Y) were first dissolved in distilled water. The solution was then dropped into an ammonium hydroxide solution (2 mol l^{-1}) under vigorous stirring. The precipitated gel was washed repeatedly with distilled water until the pH had decreased to a value below 8. After filtering, the precipitate was transferred to an alumina tube which was filled with distilled water, sealed with a cap and placed in an autoclave. Hydrothermal synthesis was performed for times up to 4 h at fixed temperatures between 100 and 300°C. After the system had been rapidly cooled, the product was washed first with dilute nitric acid and then repeatedly with distilled water. The powders used in subsequent colloidal dispersion experiments were kept in suspension prior to their use. In addition, some powders were dried for 4 h at 100°C and used for X-ray analysis and for sintering experiments on powder compacts.

The synthesized powders were characterized by X-ray diffraction (XRD) and transmission electron microscopy (TEM). Analysis of the crystal structure was performed in a diffractometer (Scintag XDS 2000) using Cu K_α radiation at a scan rate of 2° 2θ min^{-1}. Crystallite size was measured from XRD patterns at a scan rate of 0·5° 2θ min^{-1}. The crystallite size was calculated from the Scherer formula

$$D = 0{\cdot}9\lambda/(\beta \cos\theta) \quad (1)$$

where λ is the wavelength of the X-rays, θ is the diffraction angle, and β is the corrected half-width given by:

$$\beta^2 = \beta_m^2 - \beta_s^2 \quad (2)$$

where β_m is the measured half-width and β_s is the half-width of a standard CeO_2 sample with a crystal size greater than 100 nm. The reflection from the (422) plane, occurring at 88° 2θ, was used for the crystallite size measurement. Specimens of the synthesized powder for TEM (Philips EM-430T) were made by putting a drop of the suspension described earlier on a holey carbon film, followed by drying. Particle sizes were determined by measuring maximum diameters of more than 100 particles in the TEM micrographs.

2.2 Colloidal stabilization of suspensions of nanocrystalline particles

The suspensions of nanocrystalline particles were stabilized electrostatically by the adsorption of ions from solution or sterically by the adsorption of polymer molecules. For electrostatic stabilization, the pH value of the suspensions was adjusted by the addition of HNO_3 or NH_4OH to determine the range of stability. The stability of the suspensions was checked by particle size analysis (Model CAPA-700, Horiba Ltd, Kyoto, Japan). A decrease in the stability of the suspension is expected to lead to a greater tendency for flocculation of the particles, thereby producing a wider distribution of sizes. In addition, individual drops of the suspensions were placed on a glass slide and the water was evaporated. The structure of the resulting sediment was observed by scanning electron microscopy (SEM). Suspensions with pH values corresponding to good stability were heated at 70–80°C in order to increase the concentration of particles. At any pH, the concentration limit for stability was taken as that producing no visible sedimentation after 24 h.

The stabilization of the suspensions by the use of polymeric dispersants was also investigated. In the experiments, the polymers were added to dilute suspensions of the particles, after which the suspensions were concentrated by evaporation at 70–80°C. The stability of the suspensions was checked by observing the degree of sedimentation after 24 h. Dispersants which produced no visible sedimentation after 24 h were considered to be effective stabilizing agents. From these survey experiments, polyvinyl pyrrolidone (PVP) with a relative molecular weight of 30000 was found to be effective. PVP was added to the suspension at a pH of 3·5 to 4 and the concentrations of PVP and particles required to produce a stable suspension were determined.

2.3 Preparation and sintering of thin films and powder compacts

The stable suspensions were used to prepare adherent films on dense, rigid substrates by dip-coating or spin-coating. Because they were readily available, single-crystal silicon wafers were used as the substrate material in the initial experiments performed to determine the key coating parameters. Later, polycrystalline Y_2O_3-stabilized ZrO_2 was used as the substrate material for investigation of the sintering of the films. Dip-coating was performed by immersing the substrate in the suspension and manually removing it for drying. This procedure did not provide adequate control of the thickness of the coating and was replaced by spin-coating. In the process, 1–2 cm^3 of the suspension was placed on the substrate (≈3 cm square) held in the spin-coating equipment (Model 100CB, Brewer Science, Rolla, MO) and the rotational speed was increased quickly to 1000 rev min^{-1}. After the coating process, the film was dried at room temperature for 24 h.

Films were also prepared on porous Al_2O_3 substrates using the procedure described above for the coating of dense substrates. The porous substrates (porosity ≈ 30%) were prepared by tape-casting of Al_2O_3 powder (Alcoa A-1000 SG; average particle size ≈ 0·5 μm), followed by lamination, binder burnout and sintering (1 h at 1400°C). As described later, SEM of the fractured surface of the substrate revealed an average grain size of ≈2 μm and a fairly wide distribution of pore sizes.

In the sintering experiments, the adherent films were heated in air at 1°C min^{-1} to 400°C (to burn out the polymeric dispersant) and at then 10°C min^{-1} to fixed temperatures up to 1300°C. The thickness of the sintered films was determined by SEM observations of the fractured cross-sections. The microstructure of the top surface and the fractured surface of the films was also observed by SEM. The average grain size was estimated by XRD line broadening and by SEM of the fractured surfaces.

As a comparison, the sintering characteristics of compacts formed from the synthesized powder were investigated. The compacts (≈6 mm in diameter by 5 mm) were prepared by die pressing under a pressure of ≈50 MPa. Sintering was performed in air in a dilatometer at 10°C min^{-1} to 1350°C. The density of the sintered compacts was determined from the initial density and the observed shrinkage. The microstructure of fractured surfaces was observed by SEM.

3 Results

The experiments allowed an investigation of the factors controlling the characteristics of the powders prepared by the hydrothermal technique, the stability of suspensions of the nanocrystalline

particles, the preparation of thin films from the suspensions and the sintering characteristics of the films and powder compacts. The results are described separately in the following sections.

3.1 Powder characteristics

Figure 1 shows the X-ray diffraction patterns of the undoped CeO_2 powder synthesized under hydrothermal conditions of 4 h at 100, 200 and 300°C. For peaks at a given 2θ value, the area under the peak increases significantly and the half-width decreases significantly as the temperature increases from 100 to 200°C. However, the changes in the peak area and half-width are less significant as the temperature increases from 200 to 300°C. Furthermore, X-ray diffraction patterns showed no significant change in the area under the peak as the time of synthesis was increased from 4 to 8 h.

The hydrothermal process occurs by a solution–diffusion–precipitation mechanism, in which the gelatinous precipitate (produced at room temperature and atmospheric pressure) dissolves in the liquid and precipitates on the nuclei formed initially. The X-ray diffraction data of Fig. 1 indicate that, compared with the synthesis temperatures of 200 and 300°C, a significantly smaller amount of crystals is formed and the crystal size is finer at 100°C. The smaller amount of crystals indicates that the reaction is not completed after 4 h at 100°C. Furthermore, the absence of any significant change in the peak area for synthesis times longer than 4 h at 300°C indicates that the reaction is essentially completed under these conditions. Longer synthesis times lead only to coarsening of the crystals. In view of the X-ray diffraction data, a standard set of conditions of 4 h at 300°C was used in the rest of the experimental work.

A transmission electron micrograph of the CeO_2 powder synthesized for 4 h at 300°C is shown in Fig. 2. All of the particles appear to have faceted sides and this is an indication of their crystalline nature. A histogram of the distribution in particle sizes, determined from the TEM micrographs by measuring the maximum diameters of more than 100 particles, is shown in Fig. 3. The average particle size was 14 ± 3 nm, which is in good agreement with the average crystal size of 12 nm obtained by X-ray line broadening.

For the doped powder (CeO_2 doped with 6 at% Y), X-ray diffraction patterns of similar powders doped with up to 20 at% Y showed no evidence for the free Y_2O_3 phase. Furthermore, energy dispersive X-ray analysis (EDAX) in the SEM revealed the presence of Y at approximately the

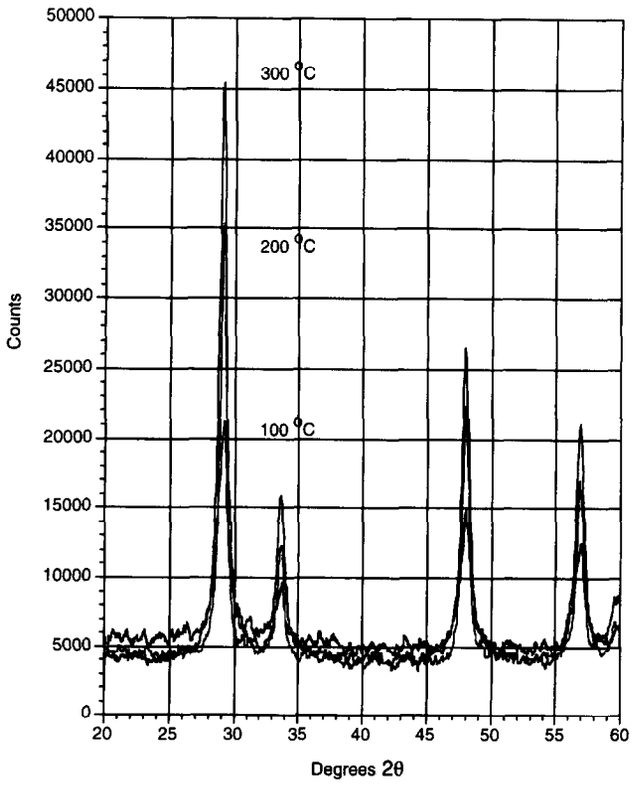

Fig. 1. X-ray diffraction patterns of the nanocrystalline CeO_2 powders synthesized by hydrothermal processing for 4 h at 100, 200 and 300°C.

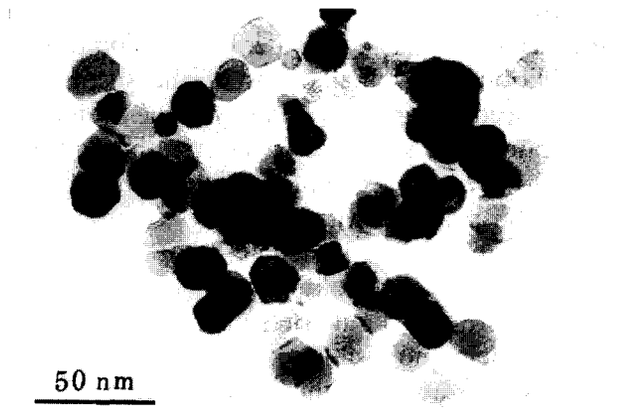

Fig. 2. TEM of the undoped CeO_2 powder synthesized by hydrothermal processing for 4 h at 300°C.

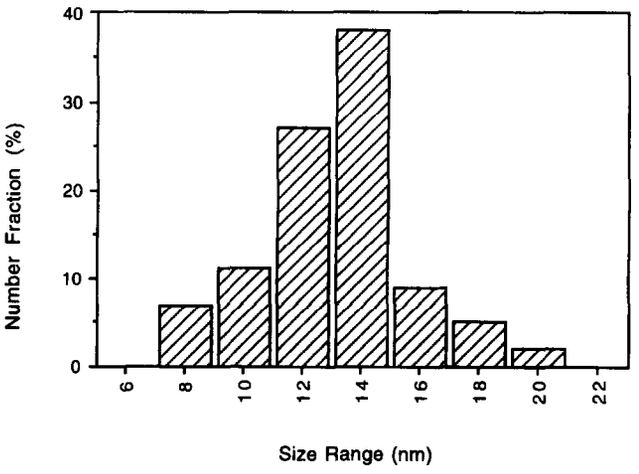

Fig. 3. Particle size distribution of the undoped CeO_2 powder measured from TEM micrographs.

required concentration in the doped powder. On the basis of these data, it may be assumed that the 6 at% Y used in the present experiments is incorporated into solid solution during the hydrothermal synthesis.

3.2 Stability of colloidal suspensions

Figure 4 shows the particle size distribution of dilute suspensions at pH values of 2·0, 4·0 and 7·4, for the CeO_2 powders doped with 6 at% Y. At pH values in the range 3·5 to 4, the average size and the spread in sizes of the particles are smallest. The data indicate that this range of pH values may provide the most stable suspensions. As the suspensions become less stable at other pH values, the particles have a tendency to flocculate, thereby increasing the average size and the distribution in sizes.

SEM micrographs of the sediment formed by placing a drop of the suspension on a glass slide and evaporating the liquid are shown in Fig. 5 for suspension pH values of 2, 4 and 7. At the pH of 7 [Fig. 5(c)] the sediment breaks up into discrete flocs of various sizes, while at a pH of 2 [Fig. 5(a)] the sediment is non-uniform and has the appearance of a two-dimensional fractal of relatively densely packed domains. The pH value of 4 [Fig. 5(b)] provides the most homogeneous structure.

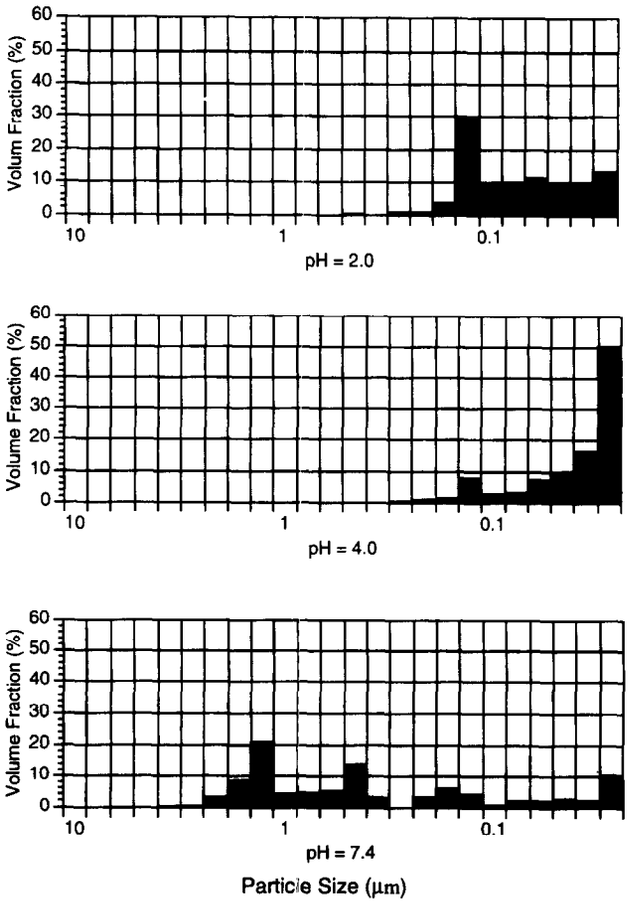

Fig. 4. Particle size distribution of the CeO_2/6 at% Y powder measured from dilute suspensions at pH values of 2·0, 4·0 and 7·4.

The structure of the film depends significantly on the stability of the suspension from which it was deposited. Stable suspensions generally lead to the production of structures with better uniformity. The data of Figs 4 and 5 indicate that, for dilute suspensions, electrostatic stabilization at a pH of 3·5 to 4 may provide a stable suspension for consolidation into a film with a fairly uniform structure. However, the concentration of the particles in the suspension also has a significant effect on the stability. Experiments with suspensions at pH values of 3·5 to 4 showed that the tendency for flocculation increased significantly above a particle concentration limit of only ≈0·2 vol%.

Higher particle concentrations were achieved by steric stabilization of the suspensions. With the use of PVP as a polymeric dispersant, particle concentrations of up to ≈10 vol% were achieved prior to flocculation. In the stabilization of

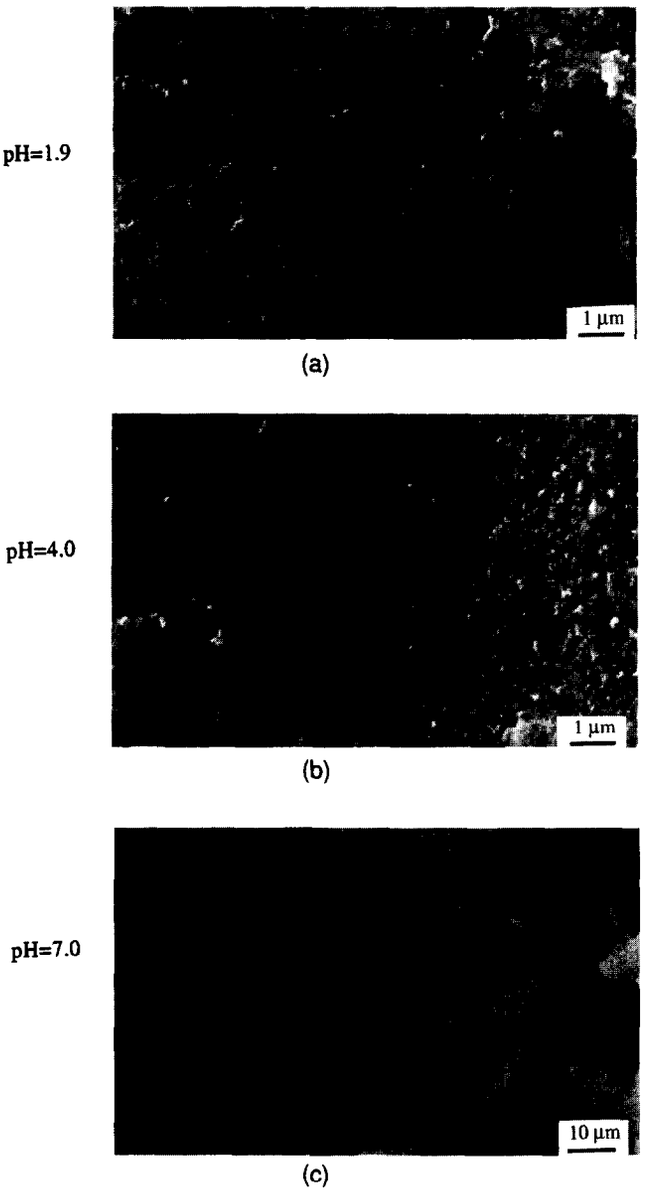

Fig. 5. SEM of the dried sediment produced from dilute suspensions of the CeO_2/6 at% Y powder at pH values of 1·9, 4·0 and 7·0.

nanocrystalline particles by polymers adsorbed on the surfaces, the very high surface area of the particles must be considered. In the experiments, it was found that ≈25 wt% of PVP (on the basis of the dry weight of the powder) was required to produce adequate stabilization of the suspensions. This high amount of polymer can be explained in terms of the very high specific surface area of the nanocrystalline powder. For the same volume (or mass) of solid, the surface area of 15 nm spheres increases by a factor of $10^3/15$ or ≈70, compared with 1 μm diameter spheres. Assuming the same surface coverage, the percentage of adsorbed polymers (as a ratio of the dry weight of the powder) required to provide effective stabilization of the nanocrystalline particles may be expected to be ≈70 times that for μm size particles.

3.3 Characteristics of thin films prepared by spin-coating

Figure 6 shows scanning electron micrographs of the top surfaces of films prepared by spin-coating from suspensions which were stabilized (a) electrostatically at a pH of 4 and (b) sterically with PVP at a concentration of 25 wt% (on the basis of the dry weight of the powder). The powder composition was that of CeO_2 doped with 6 at% Y. The surface of the film produced from the sterically stabilized suspension appears to be more uniform. This may be due to the higher particle concentration and possibly a higher degree of stability in the sterically stabilized suspensions.

For the sterically stabilized suspensions, the effect of processing parameters on the thickness and uniformity of the film prepared by spin-coating was investigated. Neglecting edge effects, the thickness of the film was uniform within the limit of measurement by SEM. Figure 7 shows the effect of the particle concentration on the thickness of the dried film prepared at a speed of 1000 rev min^{-1}. The film thickness increases with the concentration, and these data can be used effectively to prepare films of the required thickness. The effect of the rotational speed of the spin-coating equipment was also investigated. It was found that relatively slow speeds (e.g. 1000 rev min^{-1}) produced a more uniform structure.

3.4 Sintering characteristics of thin films and powder compacts

Initially, powder compacts prepared by die-pressing were sintered in a dilatometer to determine the temperature range of densification of the powders. Figure 8 shows the data for the relative density as a function of temperature for the Y-doped CeO_2 powder compacts during constant heating rate sintering at 10°C min^{-1} in air. Densification commences at ≈1000°C and almost full density is achieved by ≈1350°C. A scanning electron micrograph of the fractured surface of a compact sintered to 1350°C is shown in Fig. 9. The grain size appears fairly uniform with an average size of ≈200 nm.

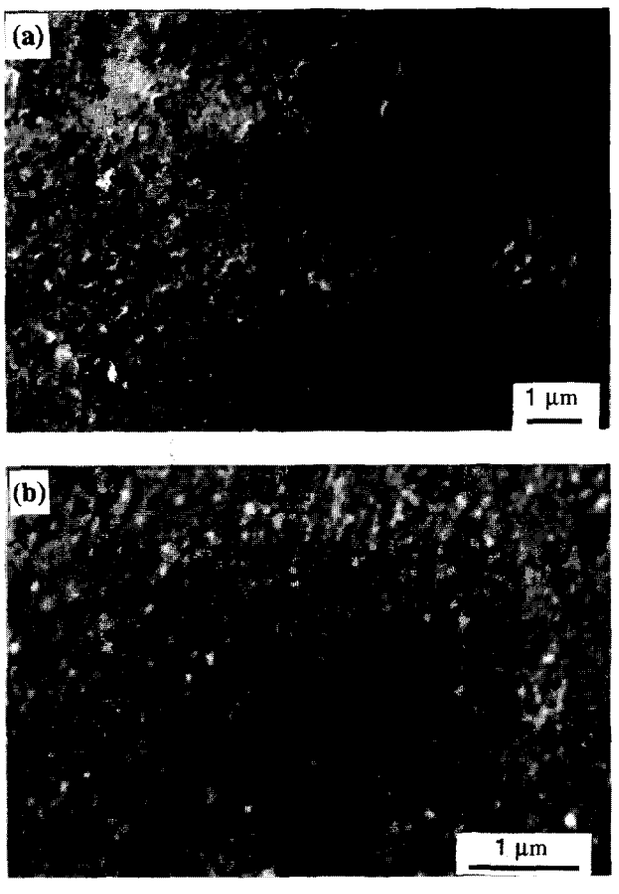

Fig. 6. SEM of the top surface of dried films prepared by spin-coating from suspensions of the CeO_2/6 at% Y powder stabilized (a) electrostatically at a pH of 4·0 and (b) sterically by polyvinylpyrrolidone (PVP).

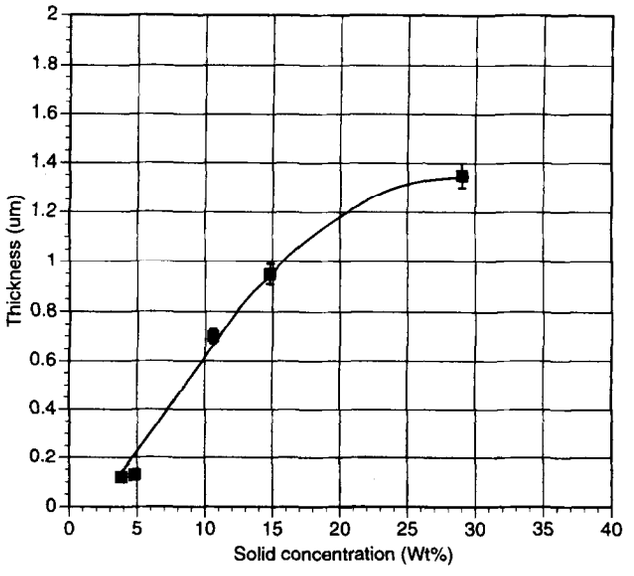

Fig. 7. Dependence of the thickness of the dried film on the concentration of particles in the suspension, for films prepared by spin-coating (1000 rev min^{-1}) of sterically stabilized suspensions.

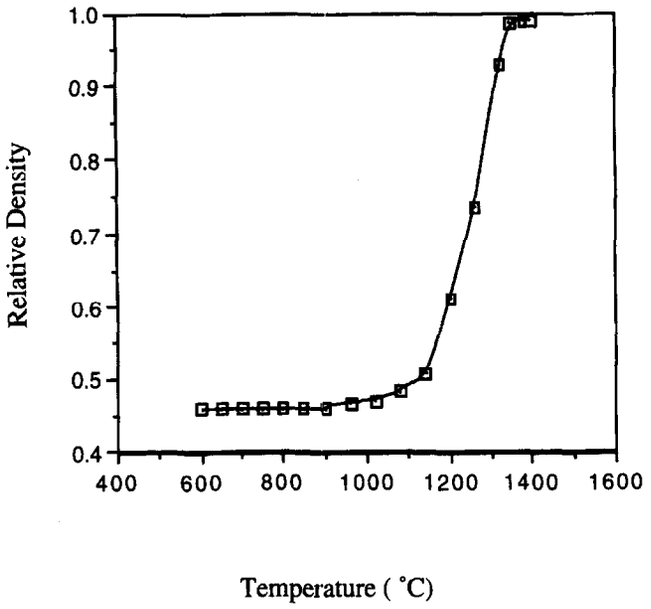

Fig. 8. Relative density versus temperature for compacts of the CeO_2/6 at% Y powder during constant heating rate sintering at 10°C min^{-1} to 1400°C.

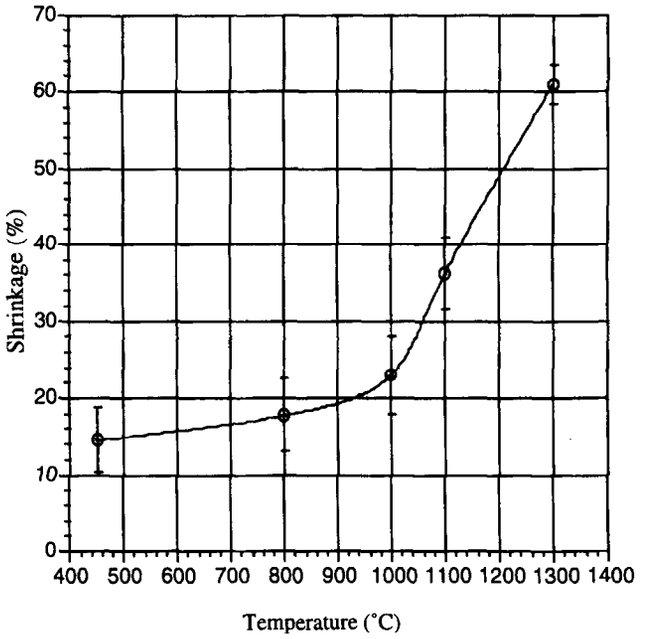

Fig. 10. Shrinkage in the thickness of the film versus temperature during constant heating rate sintering (10°C min^{-1}).

Figure 10 shows the shrinkage data for films prepared from sterically stabilized suspensions during constant heating rate sintering at 10°C min^{-1} in air. The shrinkage observed at lower temperatures (<500°C) is caused by burnout of the polymeric stabilizer (PVP). The trend in the shrinkage at higher temperatures is approximately similar to that observed in Fig. 8 for the powder compact.

Figures 11(a) and 11(b) show scanning electron micrographs of the top surface and the fractured surface of the dried film prepared from the sterically stabilized suspensions of Y-doped CeO_2 powder. The corresponding micrographs for the top surface and the fractured surface of the film after firing at 10°C min^{-1} to 1300°C are shown in Figs 11(c) and 11(d). The uniformity of the films is fairly evident. Furthermore, the sintered films appear to be almost fully dense.

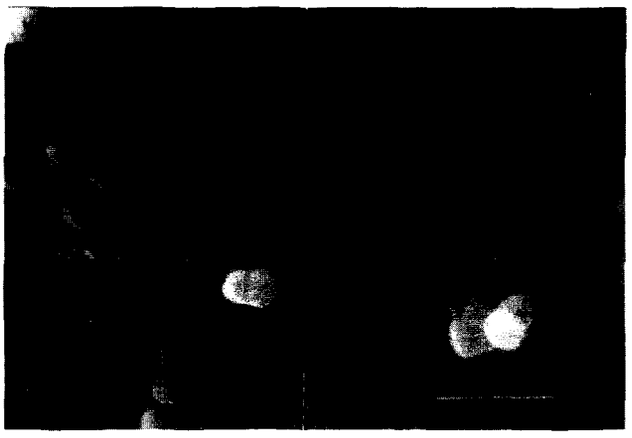

Fig. 9. SEM of the fractured surface of a powder compact (CeO_2/6 at% Y) after sintering at 10°C min^{-1} to 1350°C.

For the films prepared on porous Al_2O_3 substrates, Fig. 12 shows scanning electron micrographs of the uncoated Al_2O_3 substrate and of the top surface and the fractured surface of the film after sintering at 10°C min^{-1} to 1300°C. In spite of the very porous nature of the substrate, there is no evidence of intrusion of the suspension into the substrate. The top surface appears fairly uniform. However, cracking of the film is evident. It is believed that the cracks are due to thermal expansion mismatch between the substrate and the film during cooling from the sintering temperature.

4 Discussion

In the hydrothermal synthesis experiments, typically about 3 to 5 g of powder was produced in a liquid volume of ≈ 50 cm^3. Taking into account the theoretical density of CeO_2 (7·13 g cm^{-3}), the conditions existing during the hydrothermal process approximate those of dilute precipitates in a liquid medium. It is interesting, therefore, to determine whether the characteristics of the synthesized particles can be described by the classical theory of Ostwald ripening developed by Greenwood,[25] Wagner,[26] and Lifshitz and Slyozov[27] (often referred to as the LSW theory). According to the LSW theory, for dilute concentrations of precipitates, if the solubility of the precipitates in the medium or the deposition of the solute on the particle surfaces (i.e. the interface reaction) is rate-controlling, the size distribution function of the precipitates is time-invariant and is given by:

$$f(s) = \frac{s}{(2-s)^5}\exp\left(\frac{-3s}{2-s}\right) \quad \text{for } 0 < s < 2$$
$$f(s) = 0 \quad \text{for } s > 2 \tag{3}$$

In eqn (3), s is the reduced size of the particle, equal to R/R^*, where R is the particle radius and R^* is the size of the particles which neither grow nor shrink. R^* is related to the average particle radius, $\langle R \rangle$, according to: $\langle R \rangle = (8/9)R^*$. When the diffusion of the dissolved atoms in the solution controls the coarsening rate, the size distribution function takes the form:

$$f(s) = s^2\left(\frac{3}{3+s}\right)^{7/3}\left(\frac{3/2}{3/2-s}\right)^{11/3}\exp\left(\frac{-s}{3/2-s}\right) \quad \text{for } 0 < s < 3/2 \tag{4}$$
$$f(s) = 0 \quad \text{for } s > 3/2$$

In this case, the average radius, $\langle R \rangle$, is equal to R^*. Figure 13 shows that the particle size data for CeO_2 (histogram) follow approximately the predicted curve for Ostwald ripening controlled by diffusion through the liquid medium. It is also interesting to note that the particles have a fairly narrow spread in sizes. The present work provides an example of processing in which the spread in particle sizes of the starting powder is controlled and can be described by the LSW theory.

While a stable suspension of nanocrystalline particles can be produced by electrostatic stabilization, the low particle concentration which can be accommodated prior to flocculation has important consequences for the preparation of thin films. During the deposition and drying of the film, the particle concentration increases. Flocculation during the deposition and drying steps can lead to inhomogeneities in the structure of the dried film as well as non-uniformities in the thickness of the film. Table 1 gives the energies associated with the important surface and hydrodynamic forces acting on the particles in suspension.[28,29] The kinetic energy of sedimentation for 100 nm size particles is much smaller than that for μm size particles (1–10 μm). Sedimentation of the individual particles should not be possible, because the energy associated with the Brownian motion is significantly higher. The strongest attraction comes from the van der Waals' forces, which is associated with an energy of ≈ 10 kT, a value that is 10 times higher than that associated with the Brownian motion. To overcome the van der Waals' attraction, electrostatic repulsion[30] could be manipulated to produce repulsive potential energies of ≈ 100 kT. By changing the pH of the suspension, a stabilized suspension can be formed in which there

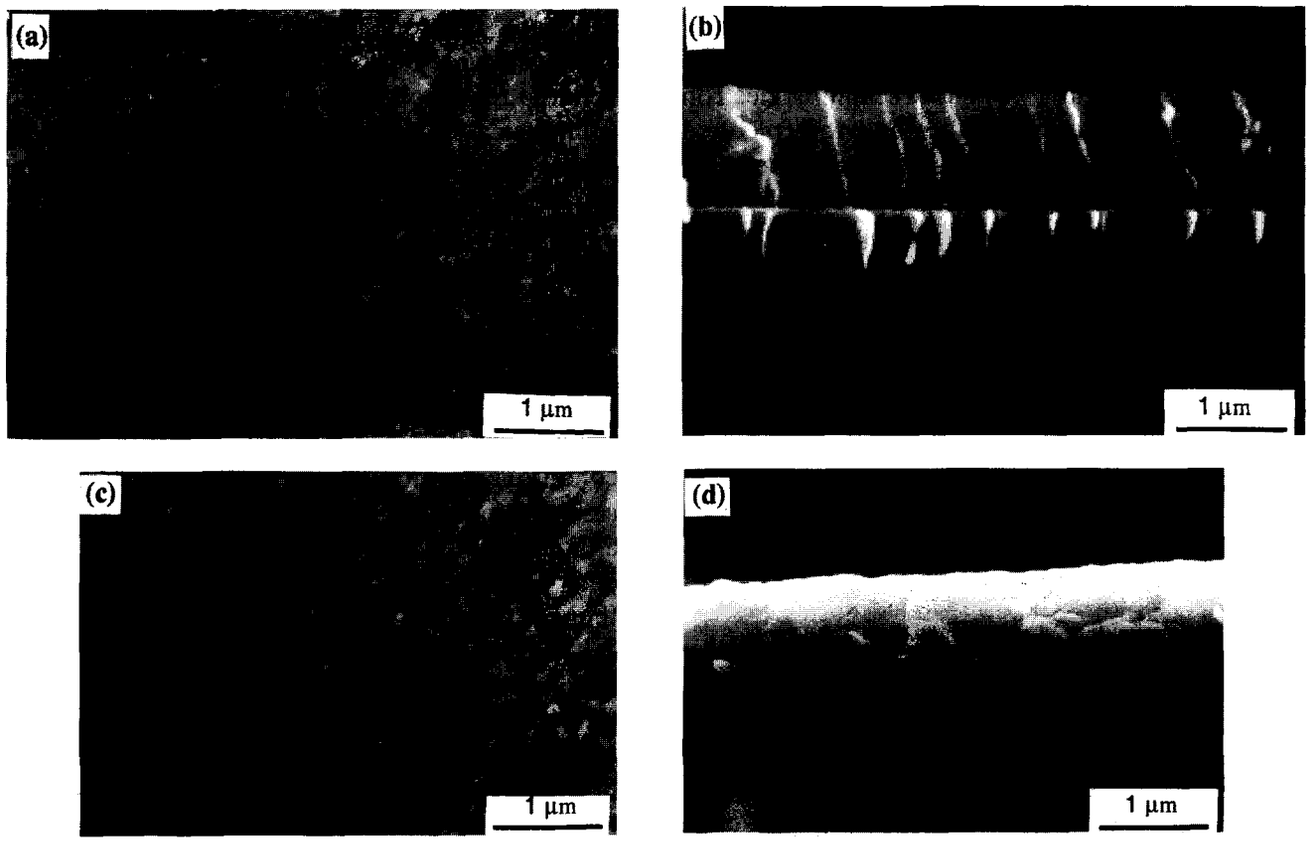

Fig. 11. SEM of (a) the top surface and (b) the fractured surface of a dried film prepared from sterically stabilized suspensions of the Y-doped CeO_2 powder. The top surface and the fractured surface of the film sintered at 10°C min^{-1} to 1300°C are shown in (c) and (d), respectively.

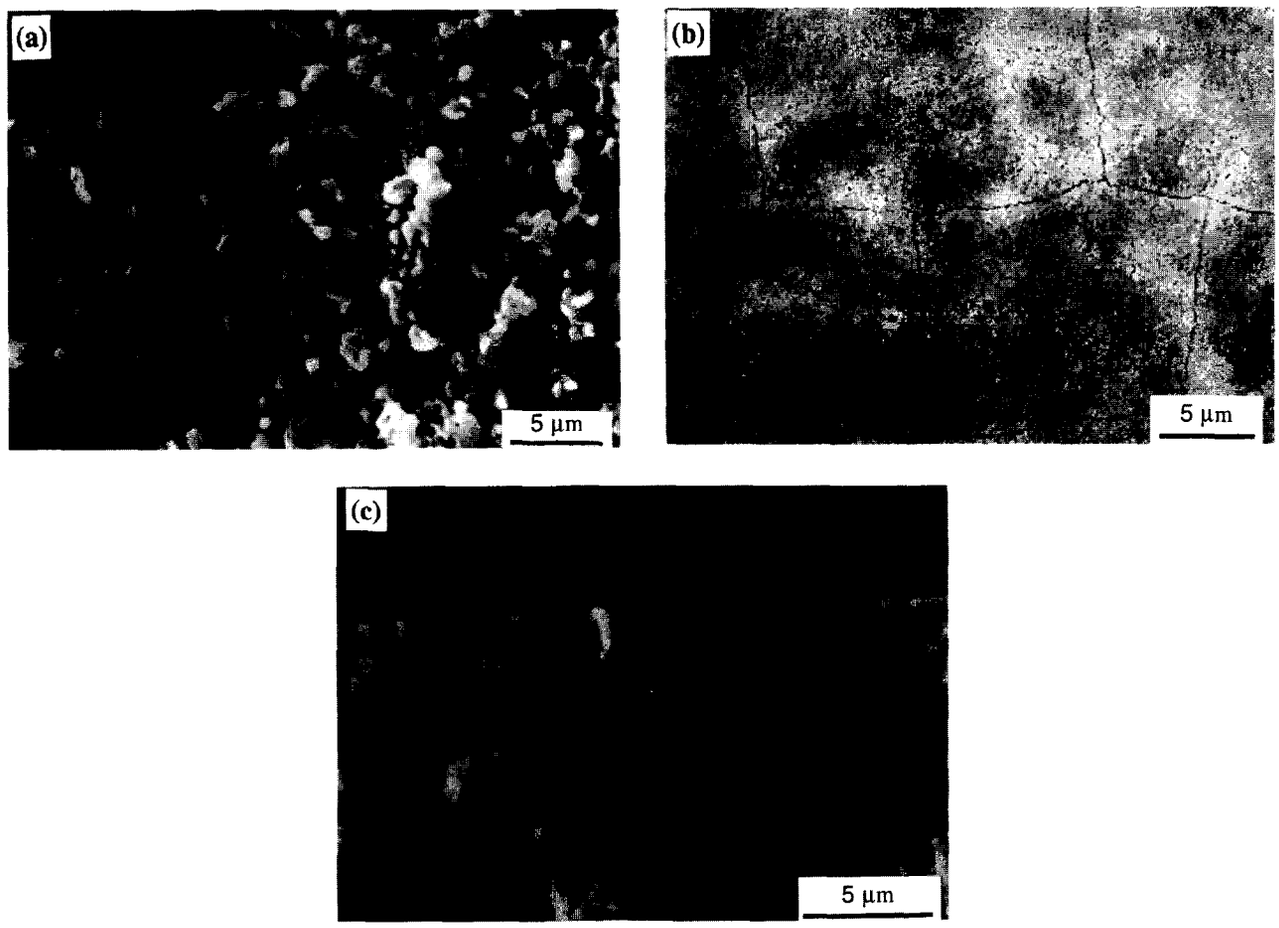

Fig. 12. SEM of (a) the uncoated porous Al_2O_3 substrate, (b) the top surface of the fired film prepared by spin-coating on the porous substrate and (c) the fractured surface of the fired film on the porous substrate.

is no sedimentation within a few days. However, as the suspension becomes more concentrated during the preparation of the film, flocculation will result. Such flocculation can take the form of different structures. Figure 14 illustrates schematically the variety of flocculated structures that can form in the suspension.[29] These particle structures can remain in suspension but will lead to inhomogeneities in the packing of the film [Fig. 6(a)].

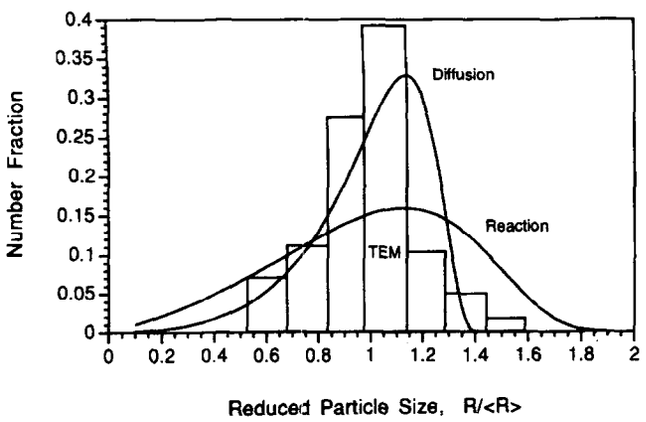

Fig. 13. Particle size distribution of the undoped CeO_2 powder (histogram) compared with the predictions of the LSW theory for matter transport controlled by diffusion and by interfacial reaction. The number fraction of particles is plotted versus the reduced particle size, equal to the ratio of the actual particle size, R, to the average particle size, $\langle R \rangle$.

For a polymer consisting of N monomer units and a monomer chain length of L, the root mean square (RMS) end-to-end distance of the polymer is equal to $N^{1/2}L$. If the RMS end-to-end distance is taken as the approximate diameter, D, of the adsorbed polymer on the particle surfaces, then for PVP with a relative molecular weight of 30 000 and $L \approx 0{\cdot}2$ nm, $D \approx 3$ nm. The particles can approach as close as $\approx 2D$ (6 nm) before the steric repulsion comes into effect. Compared with the electrostatic stabilization discussed earlier (where the separation distance is typically ≈ 50 nm), this close approach means that a greater concentration of particles can be accommodated into the suspension without causing flocculation. In this case, assuming that the particles can approach as close as ≈ 6 nm, the volume fraction of particles (approximated as spheres with a diameter of ≈ 15 nm) which can be accommodated in suspension prior to flocculation is $\approx (15/21)^3/2$ or ≈ 20 vol%, a value that is in reasonable agreement with the observed value of ≈ 10 vol%.

The results of the present work indicate that polymeric stabilization of suspensions of nanocrystalline particles provides a useful approach for the preparation of thin films. As Fig. 6 shows, the film prepared from the suspension stabilized with

Table 1. Energies of particles in suspension due to various interactions as a function of particle size (from Ref. 28)

Type of interaction	*Energy (in units of kT) for particle interactions*		
	100 nm (0·1 μm)	*1000 nm (1 μm)*	*10000 nm (10 μm)*
Van der Waals' attraction	≈10	≈100	≈1000
Electrostatic repulsion	0–100	0–1000	0–10000
Brownian motion	1	1	1
Kinetic energy of sedimentation	10^{-13}	10^{6}	10
Kinetic energy of stirring	≈1	≈1000	$\approx 10^{6}$

PVP is considerably more uniform than that prepared from the electrostatically stabilized suspensions. Because of the good stability and relatively high particle concentration, no significant changes are likely in the coating and drying steps. However, as outlined earlier, due to the very high specific surface area of nanocrystalline powders, a relatively large amount of polymer is required to provide good surface coverage on the particles for effective stabilization.

During the sintering of the films prepared from the sterically stabilized suspensions, the densification and grain growth kinetics appear to closely follow those for the sintering of powder compacts. After sintering at 10°C min^{-1} to 1300°C, films of CeO_2 doped with 6 at% Y are almost fully dense and have a grain size of ≈0·1 μm. As discussed

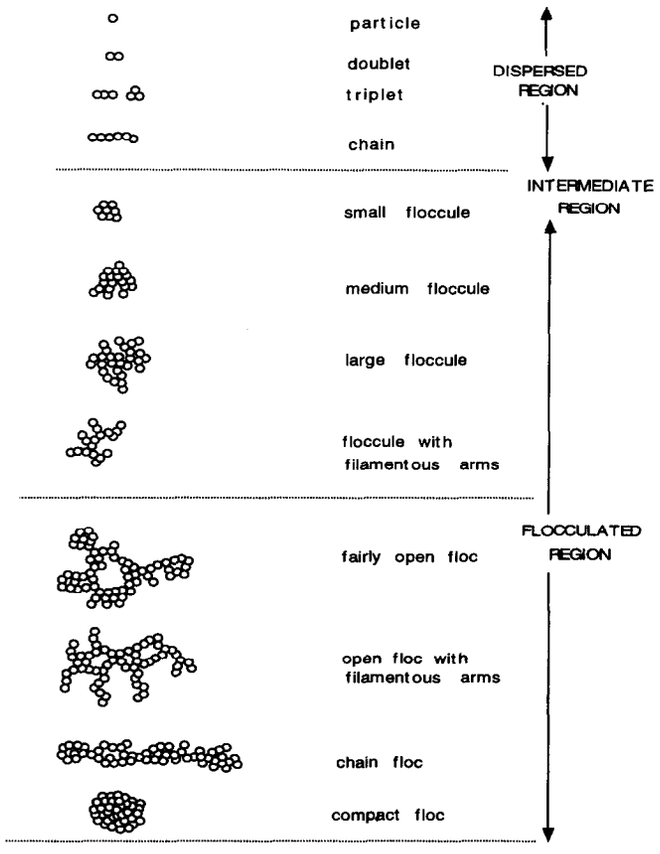

Fig. 14. Schematic diagram of the variety of floc structures that may exist in suspensions of a nanocrystalline powder (from Ref. 29).

elsewhere,[31] the use of dopants (as in the present experiments) coupled with more careful optimization of the heating schedule may provide further benefits for microstructural control of nanocrystalline ceramics.

The approach employed in the present work, in which films are produced from sterically stabilized suspensions of nanocrystalline particles, can provide significant fabrication advantages. The low sintering temperatures enlarge the compositions of substrates which can be coated without any significant interfacial reaction during sintering. Furthermore, compared with the sintering of amorphous films, the sintering of the nanocrystalline powders does not involve the nucleation and growth of crystals. The crystals are already present in the form of particles. The absence of the nucleation and growth process may allow better control of the microstructural evolution (e.g. grain size) during the firing process.

5 Conclusions

Nanocrystalline powders of CeO_2 and Y-doped CeO_2 (particle size 10–15 nm) prepared by the hydrothermal process have a fairly narrow particle size distribution which can be described by the LSW theory for Ostwald ripening controlled by the diffusion through the liquid. While electrostatic stabilization and steric stabilization (with PVP) are both effective for stabilization of the nanocrystalline particles in suspension, a significantly higher concentration of particles can be incorporated into the sterically stabilized suspension prior to flocculation. The higher concentration is due to the shorter range of repulsion between the stabilizing polymers, which allows a closer interparticle separation without flocculation. However, the high surface area of the nanocrystalline powders requires the use of a fairly high volume fraction of polymers for effective steric stabilization. The thickness of the films prepared by spin-coating from the sterically stabilized suspensions (coating area ≈3 cm square) can

be controlled by the particle concentration in the suspension and the speed of rotation of the spin-coating device. Dried films of up to ≈ 1 μm thick can be prepared in a single coating without cracking. Films of CeO_2 doped with 6 at% Y with almost full density, coupled with a grain size of $\approx 0{\cdot}1$ μm, can be produced by sintering at 10°C min^{-1} to 1300°C. The preparation of films from stabilized suspensions provides the advantages of relatively low temperature sintering, the production (in a single coating) of films with thicknesses in the range of a few tenths to 1 μm, and the coating of dense as well as porous substrates.

References

1. Uhlhorn, R. J. R., Huis in't Veld, M. J., Keizer, K. & Burggraaaf, A. J., High perm-selectivities of microporous silica-modified γ-alumina membranes. *J. Mater. Sci. Lett.*, **8** (1989) 1135–1138.
2. Zaspalis, V., Keizer, K., van Ommen, J. G., Ross, J. R. H. & Burggraaf, A. J., Ceramic membranes as catalytic active materials in selective (oxidative) dehydrogenation reactions. *Proc. Br. Ceram. Soc.*, **43** (1989) 103–107.
3. Hsieh, H. S., New membrane materials and processes for separation. *AIChE Symp. Ser.*, **84** (1988) 1–8.
4. Minh, N. Q., Ceramic fuel cells. *J. Am. Ceram. Soc.*, **76**[3] (1993) 563–588.
5. Dessauer, J. H. & Clark, H. E. (eds), *Xerophotography and Related Processes*. Focal Press, London, 1965.
6. Bos, L., Performance of thin-film chip resistors. *IEEE Trans. Components, Packaging, and Manufacturing Technol.*, **17A**[3] (1994) 359–365.
7. Weider, H., Lavenberg, S. I., Fan, G. J. & Burn, R. A., Thermomagnetic remanence writing on europium oxide. *J. App . Phys.*, **42** (1971) 3458–3462.
8. Bauer, E. G., Dodson, B. W., Ehrlich, D. J., Feldman, L. C., Flynn, C. P., Geis, M. W., Harbison, J. P., Matyi, R. J., Peercy, P. S., Petroff, P. M., Phillips, J. M., Stringfellow, G. B. & Zangwill, A., Fundamental issues in heteroepitaxy — a Department of Energy, Council on Materials Science panel report. *J. Mater. Res.*, **5**[4] (1990) 852–894.
9. Holland, L., *Vacuum Deposition of Thin Films*. Wiley, New York, NY, 1956.
10. Chopra, K. L. & Kaur, I., *Thin Film Device Applications*. Plenum Press, New York, NY, 1983.
11. Kaue, I., Pandya, D. K. & Chopra, K. L., Growth kinetics and polymorphism of chemically deposited cadmium sulfide films. *J. Electrochem. Soc.*, **127**[4] (1980) 943–948.
12. Chopra, K. L., Kainthla, R. C., Pandya, D. K. & Thakoor, A. P., Chemical solution deposition of inorganic films. *Phys. Thin Films*, **12** (1982) 167–235.
13. Lowenheim, F. A. (ed.), *Modern Electroplating*. Wiley, New York, NY, 1974.
14. Lowenheim, F. A. (ed.), *Electroplating*. McGraw-Hill, New York, NY, 1987.
15. Giess, E. A. & Ghez, R., *Epitaxial Growth, Part A*, ed. J. W. Matthews. Academic Press, New York, NY, 1975, pp. 183–213.
16. Jones, R. W., *Fundamental Principles of Sol–Gel Technology*. Institute of Metals, London, 1989.
17. Miller, K. T. & Lange, F. F., Highly oriented thin films of cubic zirconia on sapphire through grain growth seeding. *J. Mater. Res.*, **6**[11] (1991) 2387–2392.
18. Miller, K. T., Lange, F. F. & Marshall, D. B., The instability of polycrystalline thin films: experiment and theory. *J. Mater. Res.*, **5**[1] (1990) 151–160.
19. Haggerty, J. S., Growth of precisely controlled powders from laser heated gases. In *Ultrastructure Processing of Ceramics, Glasses and Composites*, eds L. L. Hench & D. R. Ulrich. Wiley, New York, NY, 1984, pp. 353–366.
20. Kodama, T. & Tamaura, Y., Reaction condition for the synthesis of ultrafine particles of the high-vacancy-content Zn(II)-bearing ferrites from iron (III) tartrate solution. *J. Am. Ceram. Soc.*, **78**[5] (1995) 1335–1342.
21. Birringer, R., Gleiter, H., Klein, H.-P. & Marquardt, P., Nanocrystalline materials: an approach to a novel solid structure with gas-like disorder. *Phys. Lett.*, **102A** (1984) 365–369.
22. Tani, E., Yoshimura, M. & Somiya, S., Formation of ultrafine tetragonal ZrO_2 powder under hydrothermal conditions. *J. Am. Ceram. Soc.*, **66**[1] (1983) 11–14.
23. Somiya, S., Hydrothermal preparation and sintering of fine ceramic powders. *Mater. Res. Soc. Symp. Proc.*, **24** (1984) 255–271.
24. Zhou, Y. C. & Rahaman, M. N., Hydrothermal synthesis and sintering of ultrafine CeO_2. *J. Mater. Res.*, **8**[7] (1993) 1680–1686.
25. Greenwood, I. W., The growth of dispersed precipitates in solutions. *Acta Met.*, **4** (1965) 243–248.
26. Wagner, C., Theorie der alterung von niederschlägen durch umlösen. *Z. Elektrochemie*, **65** (1961) 581–591.
27. Lifshitz, I. M. & Slyozov, V. V., The kinetics of precipitation from supersaturated solid solutions. *J. Phys. Chem. Solids*, **19** (1961) 35–50.
28. Warren, L. J., The stability of suspensions. *Chem. Australia*, **44**[12] (1977) 315-318.
29. Warren, L. J., Ultrafine particles in flotation. In *Principles of Mineral Flotation*, Wark Symposium, Vol. 40. Australian Institute of Mining & Metallurgy, Adelaide, Australia, 1984, pp. 185–213.
30. Wiese, G. R. & Healy, T. W., Effect of particle size on colloid stability. *Trans. Faraday Soc.*, **66**[2] (1970) 490– 499.
31. Zhou, Y. C. & Rahaman, M. N., Effect of solid solution additives on the sintering of ultrafine CeO_2 powders. *J. Eur. Ceram. Soc.*, **15**[10] (1995) 939–950.